International Journal of Applied Mathematics
Volume 38 No. 6s, 2025
ISSN: 1311-1728 (printed version); ISSN: 1314-8060 (on-line version)

BLOCKCHAIN ENABLED FEDERATED LEARNING BASED PRIVACY PRESERVED HEALTHCARE CLASSIFICATION USING FRACTIONAL FOOTBALL OPTIMIZATION ALGORITHM DRIVEN DEEP LEARNING

Neha Kudu, Dr. Manuj Joshi,

Research Scholar, Pacific Academy of Higher Education and Research University, Udaipur, Rajasthan, India. neha.kudu@vit.edu.in

Associate Professor, Faculty of Engineering, Pacific Academy of Higher Education and Research University, Udaipur, Rajasthan, lndia. manujjoshi@gmail.com

Abstract

Privacy preserved healthcare classification involves classifying the medical data, ensuring security of sensitive patient information. Blockchain enabled Federated Learning (FL) is emerging paradigm with data privacy, and security across decentralized healthcare systems. However, challenges such as scalability limitations and increased latency are observed. To eradicate these issues, Fractional Football Optimization Algorithm based Deep High-order Attention Neural Network (FFbOA_DHA-Net) is proposed for healthcare classification. Firstly, local training is done at each local node using local data. In training model, the input image is acquired initially and then pre-processing is done by midpoint filter. Further, lesion segmentation is done using TBConvL-Net, and next feature extraction is performed. Finally, healthcare classification is done using DHA-Net, that is trained by FFbOA. Here, FFbOA is designed by merging Football Optimization Algorithm (FbOA) and Fractional Calculus (FC). Moreover, weights from various local training model are aggregated and averaged in global server. Next, global model is applied on every local node based on averaged weights. Furthermore, performance of FFbOA_DHA-Net is assessed with metrics like, Mean Squared Error (MSE), Mean Average Precision (MAP), F1-measure, Root Mean Squared Error (RMSE), and loss, that attained superior values of 0.156, 96.81%, 95.75%, 0.395, and 0.034.

Keywords: Blockchain, Federated Learning, midpoint filter, Football Optimization Algorithm, Fractional Calculus.

1. Introduction

Smart healthcare is emerging as fastest developing technologies, offering significant potential for efficient and accurate prevention of various diseases. Internet of Medical Things (IoMT) comprises connected ecosystem of health systems, medical services, as well as medical devices. IoMT facilitates communication, connection, and exchange of Electronic Medical Records (EMRs) among multiple healthcare entities [1] [2]. As EMRs have highly sensitive patient information, the utilization of IoT technologies in healthcare raises serious concerns in terms of data protection. These concerns are more critical while dealing with patient specific information, and hence data security and privacy preservation are prevailing as one of the major concerns in smart healthcare domain [2]. A robust privacy preservation

International Journal of Applied Mathematics
Volume 38 No. 6s, 2025
ISSN: 1311-1728 (printed version); ISSN: 1314-8060 (on-line version)

mechanism is crucial to safeguard patient identities, financial information, medical histories, and ongoing diagnoses and treatments. The lack of reliable and efficient privacy solutions remains as a key reason for patients' reluctance to adopt e-healthcare services, as many do not trust the security and privacy mechanisms provided by service providers [3]. Blockchain technology offers decentralized trust model with many mechanisms that is capable of addressing lack of trust. Based on the concept of securely shared data, the blockchain enables data source authentication and ensures data integrity through its tamper-resistant architecture [4]. While combined with FL, blockchain enhances privacy by preventing unauthorized access to client data. In FL, the local data remains on client's device, and then updates of model are shared. This significantly preserves the privacy reducing the transmission and storage overhead [5] [6].

FL is the Artificial Intelligence (AI) paradigm enabling multiple nodes to collectively learn from shared model while keeping the data localized. It operates by allowing individual model training on decentralized and independent IoMT data [7] [8]. Each user device trains model locally by their own data, and resulting parameters of model are sent to global server, where they are aggregated. This procedure is repeated over multiple iterations till producing high quality global model. FL supports decentralized and collaborative training and is adaptable to wide range of data types [9] [10]. Although the raw training data prevails on local devices and is not uploaded to central server, the communication of model parameters introduces potential vulnerabilities. Hence, encryption techniques are employed for safeguarding model updates. Also, it is recommended that FL optimization algorithms are designed with privacy and security mechanisms [10]. This enables multiple entities, like hospitals or clinics to train global model without directly sharing sensitive data. This is achieved by distributing initial model to participants, and then return their locally trained parameters for aggregation. Since data never leaves local device, FL offers stronger privacy protections compared to traditional centralized training methods [5]. This enables diverse applications, including Electronic Health Records (EHR) management, IoMT systems [11] [10], wearable health monitoring [12] [10], and medical imaging analysis [13] [10]. The growing adoption of digital healthcare applications based on IoMT reflects the increasing reliance on connected medical devices, and wireless technologies throughout healthcare networks [8].

IoMT provides wide range of applications to support digital healthcare applications and is often referred as the IoT-enabled digital healthcare system. These application leverages IoT services to provide ubiquitous, real-time health monitoring, thus enabling users to track their health conditions [8]. Medical images, which has highly sensitive patient information pose significant risks while shared or stored through centralized systems, as they are vulnerable to unauthorized access and data breaches. Hence, ensuring privacy and security in medical image analysis is crucial for maintaining patient trust and complying with the data protection regulations [14] [15]. Advanced imaging techniques, like Chest X-rays (CXR) and Computed Tomography (CT) plays critical role in diagnosing various types of infections. To enhance the accuracy of such diagnostics, numerous Deep Learning (DL) models are developed to analyse CT and CXR images and identify multiple infections [16]. As a core component of

AI, Machine Learning (ML) technologies [17] [18] are extensively adopted in healthcare sector for applications, like health monitoring and disease diagnosis. In particular, DL shows strong potential in automated detection of COVID-19 and other chest diseases through analysis of diagnostic images, especially CXR [18] [19]. The ML and DL techniques are demonstrated with remarkable capabilities in accurately identifying disease patterns from medical images, even when trained on limited number of infected samples [4]. Deep Neural Network (DNN), widely recognized for their effectiveness in general image classification tasks are playing a pivotal role in improving diagnostic accuracy and efficiency in medical imaging [18].

Main objective of this work is Blockchain enabled FL based privacy preserving healthcare classification by FFbOA_DHA-Net. Initially, the local training is conducted on each node by its respective local data. Here, weights of model from each node are aggregated after training and then averaged on blockchain enabled global cloud server, ensuring integrity and transparency. Then, updated global model is distributed to all local nodes, where it is utilized for refining local models based on the newly averaged weights. In local training phase, the healthcare classification process involves several key steps including: initial acquisition of input image is done and then pre-processing is carried out by midpoint filter. Further, lesion segmentation is carried out using TBConvL-Net model, and next extraction of features are performed. Lastly, classification is done using DHA-Net, where DHA-Net is tuned by FFbOA. Herein, FFbOA is formed by combination of FbOA with FC to enhance the optimization performance.

The novel contribution is given as below,

- **Developed FFbOA_DHA-Net for privacy preserving healthcare classification:** Privacy preserving healthcare classification is done in blockchain enabled FL using DHA-Net. This DHA-Net is trained by FFbOA, that is formed by hybridization of both FbOA and FC.

Remaining sections comprises: Section 2 involves literature works of traditional approaches, section 3 introduces FFbOA_DHA-Net for privacy preserving healthcare classification, section 4 describes result with discussion, and section 5 concludes the work.

2. Motivation

Privacy preserved healthcare classification is required to leverage advanced data-driven technologies in medical diagnosis while ensuring the confidentiality of sensitive patient information. With increasing adoption of digital healthcare systems and IoMT, vast amounts of personal health data are continuously generated and analyzed. However, centralized data storage and processing creates significant risks, including unauthorized access, and non-compliance with protection regulations. These concerns have led to reduced patient trust and hesitancy in sharing critical health information. Therefore, developing secure and privacy-preserving classification methods is essential to enable accurate medical analysis, and foster trust among patients.

International Journal of Applied Mathematics
Volume 38 No. 6s, 2025
ISSN: 1311-1728 (printed version); ISSN: 1314-8060 (on-line version)

2.1 Literature Survey

A. lakhan, *et al.* [8] developed FL-based blockchain-enabled task scheduling (FL-BETS) framework for healthcare. This model effectively identified security and privacy issues while consuming minimal resources. However, it did not account for dynamic and run-time unknown attacks, limiting its ability to ensure comprehensive privacy preservation. G. C. Amaizua, *et al.* [15] designed FL combined with Vision Transformers and blockchain technology (FedViTBloc) for medical image analysis. This model had robustness against vulnerabilities and ensured data privacy, but the energy consumption and scalability of blockchain were not optimized. H. Malik, *et al.* [4] modelled Capsule network (CapsNet) with incremental extreme learning machines (IELMs) for classification of COVID-19 using CT scans. This technique enabled data sharing while preserving anonymity and enhanced the overall generalization performance compared to single-site models. However, it was not well-suited for disease classification using sonography and CXR images. V. Stephanie, *et al.* [5] presented Privacy-preserving blockchain-based ensemble-integrated FL scheme in healthcare system. Here, few amounts of time were consumed during blockchain smart contract execution and ensemble weights training. Nevertheless, this model failed in considering model heterogeneity and heterogeneous tasks at hospital participant's level.

R. Saidi, *et al.* [19] introduced Multi-classification FL method enhanced by blockchain technology for chest disease classification. This scheme addressed several critical challenges in medical diagnostics with better privacy concerns. However, it failed to address the complexities of regulatory frameworks and ensured compliance across different jurisdictions. G. Bian, *et al.* [6] developed Efficient trusted FL scheme for COVID-19 detection. Even though this model was robust with short training time and high detection accuracy, it did not enhance the robustness along with privacy and also was not extended to different medical fields. H. Malik, *et al.* [18] designed Decision-making-based FL network (DMFL_Net) + DenseNet-169 model for classification of COVID-19 from multiple chest diseases using X-rays. This approach effectively safeguarded data privacy across diverse clients. However, it failed to exhibit the ability to exchange patient records freely and train vision transformers to evaluate various privacy preserving policies. R. Durga and E. Poovammal., [20] modelled FL Ensembled Deep five learning blockchain model (FLED-Block) for COVID-19 prediction. This model effectively preserved data privacy among heterogeneous users; however, it failed to reduce the blockchain latency and did not optimize cost effectiveness of solution.

2.2 Challenges

The challenges experienced by traditional approaches on blockchain enabled FL based privacy preserved healthcare classification are as below,

- The FL-BETS framework, introduced in [8], was designed to address privacy and security concerns while minimizing resource consumption. But it struggled to support learning across distributed medical facilities and failed to enhance fairness in medical image classification.

ISSN: 1311-1728 (printed version); ISSN: 1314-8060 (on-line version)

- In [15], the FedViTBloc method was employed to enhance system trustworthiness. However, it frequently encountered challenges with data diversity and scalability, limiting its ability to develop universally robust diagnostic models.
- CapsNet with IELMs in [4] achieved high accuracy for classification of COVID-19 by CT scans. However, it failed in effectively identifying healthcare data due to the absence of optimized DL techniques.
- DMFL_Net combined with DenseNet-169 in [18] effectively safeguarded data confidentiality and security during medical data transfers between hospitals; however, it did not address or reduce the computational complexity associated with privacy preservation.
- The usage of ML-enabled dynamic IoMT systems, incorporating many technologies for digital healthcare applications are steadily increasing in real-world use. However, traditional learning models remain vulnerable to data fraud within distributed IoMT environments, making it a persistent and critical research challenge.

3. Proposed Fractional Football Optimization Algorithm enabled Deep High-order Attention Neural Network for privacy preserved healthcare classification

Medical data is distributed across multiple institutions and locations in decentralized healthcare systems. The maintenance and preservation of patient details for accurate diagnostic modeling remains as a significant challenge. Moreover, hacking or adversarial attacks leads to life-threatening consequences and hence implementing a robust security measure is critical in ensuring the safety and reliability of medical data. This research utilizes two technologies, namely FL and blockchain to solve these problems. The main aim of this research is blockchain enabled FL based privacy preserving healthcare classification by FFbOA_DHA-Net. Initially, local training based on local data at each node is carried out. Further, server is updated based on weights and thereafter, model aggregation is conducted at server. Next, global model is downloaded at nodes and then training is updated with respect to downloaded global model and local model. Further in training model, the healthcare classification is performed by involving following steps: Firstly, the input image is taken from dataset specified in [21]. Then, pre-processing is carried out using Midpoint filter [22] to remove noises from an input image. Thereafter, lesion segmentation is done employing TBConvL-Net [23]. Next, feature extraction is performed by considering features like Learned Invariant Feature Transform (LIFT) [24] and statistical features, namely entropy, mean and skewness [25]. Finally, the healthcare classification is conducted using DHA-Net [26], which is trained utilizing FFbOA. Here, FFbOA is designed by combining FbOA [27] and FC [28]. Figure 1 shows block diagram of FFbOA_DHA-Net for blockchain enabled FL based privacy preserving healthcare classification.

International Journal of Applied Mathematics
Volume 38 No. 6s, 2025
ISSN: 1311-1728 (printed version); ISSN: 1314-8060 (on-line version)

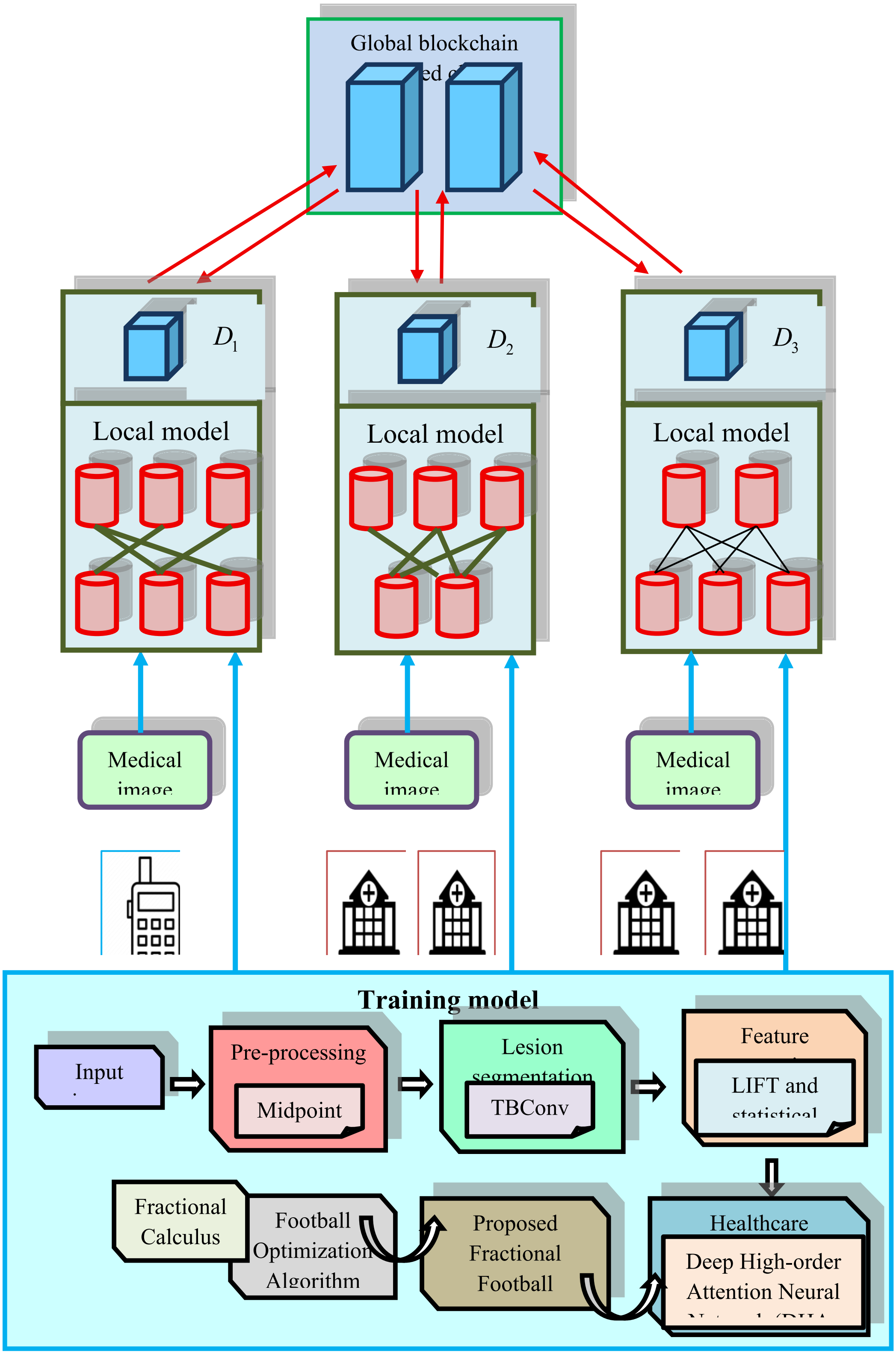

Figure 1. Block diagram of proposed FFbOA_DHA-Net for blockchain enabled FL based privacy preserved healthcare classification

Received: August 04, 2025

3.1 Local training based on local data

Local training based on local data refers to a learning paradigm, where the training process utilizes data that is stored and processed locally, typically on edge devices, local servers, or within a specific geographic or organizational boundary. In case of medical data or image, local data is available in hospitals, where patient data is locally available. This training is done at every local node and training model is explained below.

3.1.1 Training at every local node

Training at each local node refers to a decentralized approach in the learning paradigm, where each local device or system, called as node trains its own model on its own data, without sending raw data to central location. Here, local devices, like smartphones, and hospital servers collects the medical image or local data of patients and then train them using some training model. This stored data is then converted to particular weights and then updated to the central server, at which the weights are aggregated. Training local data at each node is essential for maintaining data privacy, minimizing communication overhead, and supporting real-time, personalized learning by processing information directly at its source. Instead of transmitting large volumes or sensitive raw data to a central server, each node processes and learns from its own data locally, which enhances security, complies with data regulations, and reduces latency. This decentralized approach also ensures that models are tailored to the specific context of each node, making them more effective and scalable across diverse and distributed systems.

3.1.2 Training model

Training of local data is carried out at every local node with available medical image, that is utilized for healthcare classification. This model includes various steps, like acquisition of input image, pre-processing, lesion segmenting, extraction of features, and healthcare classification. Local training model is shown in figure 2.

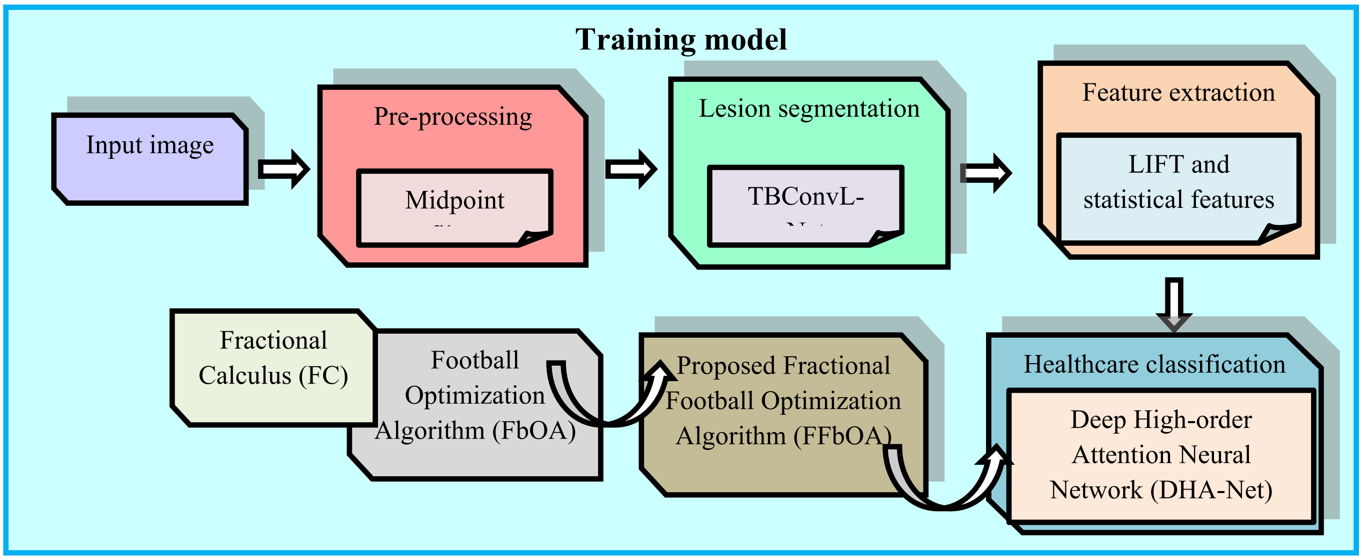

ISSN: 1311-1728 (printed version); ISSN: 1314-8060 (on-line version)

The image required for the processing is acquired from Indian Diabetic Retinopathy Image Dataset (IDRiD) [21]. This database specifies Indian population and offers pixel-level annotations of both common diabetic retinopathy lesions as well as normal retinal structures. Representation of dataset with various retinal images are given below,

$$W = \{W_1, W_2, ..., W_h, ..., W_x\} \qquad (1)$$

Herein, W denotes dataset, W_h is the input image utilized for processing, x is overall retinal images in dataset.

b) Pre-processing using midpoint filter

In this process, the noise reduction in image is done to improve quality of image. Here, pre-processing is carried out by midpoint filter [22], which is a non-linear filter based on order-statistics. The input image W_h is fed for pre-processing phase using midpoint filter. This filter slides over window size $(2F+1)W_h(2F+1)$ points over noisy input image W_h and F as an integer. Samples inside window are arranged in ascending order, and average of largest and smallest samples inside window is utilized as filter output. This filter process is formulated as below,

$$M(l,m) = \frac{1}{2}\left((\min(W_h(l+i, m+j)) + (\max(W_h(l+i, m+j))\right), -F \leq (i,j) \leq F \qquad (2)$$

wherein, $M(l,m)$ is $(l,m)^{th}$ sample of output sequence of midpoint filter M . Thus, pre-processed resultant is indicated by E_h.

c) Lesion segmentation using TBConvL-Net

The lesion segmentation process is identifying and delineating abnormal lesions within the medical images. Also, the pathological features are detected and outlined from the retinal images in case of lesion segmentation. The pre-processed image E_h is allowed for the process of lesion segmentation, that is carried out by TBConvL-Net [23].

i) Architecture of TBConvL-Net

TBConvL-Net [23] is the hybrid DL model that enhances the accuracy and robustness of medical image segmentation. This architecture has multiple key components, like encoder-decoder block, and BCon vLSTMand transformer block. TBConvL-Net architecture for lesion segmentation is expressed in figure 3.

Encoder-Decoder block: Encoder block has four stages, wherein each stage comprises dual separate convolutional layers utilizing 3×3 filters. Then, the maximal pooling layer is followed by this convolutional layer with 2×2 filters, which is then forwarded to Rectified Linear Unit (ReLU). At every stage, filter count doubles when compared with preceding stages. Finally, the high-level semantic information is extracted at the last layer. Here, the layer dimensions are gradually increasing to form high-dimensional image representations. In this block, feature maps produced by early convolutional layers are combined with current

International Journal of Applied Mathematics
Volume 38 No. 6s, 2025
ISSN: 1311-1728 (printed version); ISSN: 1314-8060 (on-line version)

layer features, and merged resultant is passed to the next convolutional layer. Densely connected convolutions offer significant advantages over conventional convolutional methods. Moreover, the danger of gradient vanishing and bursting is avoided by this network, as the densely connected convolutions are benefited from each feature. Consider $k^{a\times a}$ as depth wise separable convolution operation $(n^{a\times a})$ of kernal size $(a\times a)$ followed by batch normalization operation U on input E_h is formulated by,

$$k^{a\times a} = U(n^{a\times a}(E_h)) \qquad (3)$$

Also, consider the output of b^{th} encoder block as $V_b, b = 1,2,3$, found by utilizing dual consecutive $k^{3\times3}$ operations, followed using $b^{th}(2\times2)$ max pooling operation G on encoded features $\Im$ as,

$$V_b = G(k^{3\times3}(k^{3\times3}(\Im))) \qquad (4)$$

The encoding blocks are utilized by small spatial input sizes with $\square \times \square \times \square$ for V_1 , $\frac{1}{2}\square \times \frac{1}{2}\square \times 2\square$ for V_2 , and $\frac{1}{4}\square \times \frac{1}{4}\square \times 4\square$ for V_3 . After encoding block, the densely connected blocks are given as follows,

$$T_1 = A(k^{3\times3}(k^{3\times3}(V_3))) \qquad (5)$$

$$T_2 = S(T_1) \square\, T_1 \qquad (6)$$

$$T_3 = \left[A(k^{3\times3}(k^{3\times3}(T_2)))\right] \square\, T_1 \square\, T_2 \qquad (7)$$

wherein, A is ReLU unit, S represents Swin Transformer Block (STB), $\square$ indicates concatenation operation, and T_1, T_2, T_3 are densely connected blocks. Finally, the decoder block is formulated by,

$$T_b = C^T(k^{3\times3}(k^{3\times3}(T_3))) \square\, S(\Delta_{lstm}(V_b)) \qquad (8)$$

Herein, C^T is transposed convolution operation of b^{th} decoder block, and Δ_{lstm} is BConvLSTM. Finally, the resultant $(E_h)_{out}$ by applying dual consecutive operations $k^{3\times3}$ is indicated by,

$$(E_h)_{out} = \Re(k^{3\times3}(k^{3\times3}(T_3))) \qquad (9)$$

Bidirectional ConvLSTM and Transformer Block: Bidirectional LSTM captures contextual information, enhancing ability of network for learning complex data patterns. Swin Transformers utilizes hierarchical approach for processing nonoverlapping local image patches, making them for learning multiple scale features. This block includes input gate I_g, memory cell Y_{m_g} , forget gate F_g , as well as output gate O_g , that are formulated as below,

Received: August 04, 2025

International Journal of Applied Mathematics
Volume 38 No. 6s, 2025
ISSN: 1311-1728 (printed version); ISSN: 1314-8060 (on-line version)

$$Y_{m_g} = F_g \otimes Y_{m_{(g-1)}} + I_g \tan\square(\square_{(\aleph, Y_m)} \circ \aleph_g + \square_{(\square, Y_m)} \circ \alpha_{(g-1)} + U_{Y_m}) \tag{10}$$

$$O_g = \Re(\square_{(\aleph, O)} \circ \aleph_g + \square_{(\square, O)} \circ \alpha_{(g-1)} + \square_{(Y_m, O)} \otimes Y_{m_g} + U_O) \tag{11}$$

$$I_g = \Re(\square_{(\aleph, I)} \circ \aleph_g + \square_{(\square, I)} \circ \alpha_{(g-1)} + \square_{(Y_m, I)} \otimes Y_{m_{(g-1)}} + U_I) \tag{12}$$

$$F_g = \Re(\square_{(\aleph, F)} \circ \aleph_g + \square_{(\square, F)} \circ \alpha_{(g-1)} + \square_{(Y_m, F)} \otimes Y_{m_{(g-1)}} + U_F) \tag{13}$$

$$\alpha_g = O_g \otimes \tan\square(Y_{m_g}) \tag{14}$$

Herein, $\circ$ and $\otimes$ are convolutional and Hadamard operations, $\aleph_g$ is input tensor, α_g is output tensor, $\square_{(\aleph,*)}$ is 2D convolution mask of hidden state, $\square_{(\square,*)}$ is 2D convolution mask of input state, bias terms are U_{Y_m}, U_O, U_I, and U_F. Here, dual separate paths in forward as well as backward direction are processed in BConvLSTM, wherein forward path processes from first image to last image and backward path processes from last image to first image. Thus, the output from the BConvLSTM is formulated by,

$$\aleph_{out} = \tan\square((\square^{\alpha\rightarrow} \circ \alpha_g^{\rightarrow}) + (\square^{\alpha\leftarrow} \circ \alpha_g^{\leftarrow}) + U) \tag{15}$$

wherein, hidden state tensors are $\alpha\rightarrow$ and $\alpha\leftarrow$ in forward and backward states, hyperbolic tangent function is $\tan\square$, and U is bias component. Consider β_{in} be input to first STB and the resultant χ_1 is formed by concatenating β_{in} with first Multi head Self-Attention (MSA) module, that is given by,

$$\chi_1 = \beta_{in} \square N_l(MSA(\beta_{in})) \tag{16}$$

Here, N_l is layer norm. Further, χ_2 and χ_3 are calculated as below,

$$\chi_2 = \chi_1 \square MLP\left(N_l\left(\chi_1\right)\right) \tag{17}$$

$$\chi_3 = \chi_2 \square N_l\left(SW - MSA\left(\chi_2\right)\right) \tag{18}$$

Here, Shifted Window-based MSA is SW-MSA, and Multilayer Perceptron is MLP. Finally, output β_{out} of second STB is given by,

$$\beta_{out} = \chi_3 \square MLP(N_l(\chi_3)) \tag{19}$$

Hence, the resultant from lesion segmentation by TBConvL-Net is represented as H_h. Figure 3 shows the architecture of TBConvL-Net for segmentation purpose.

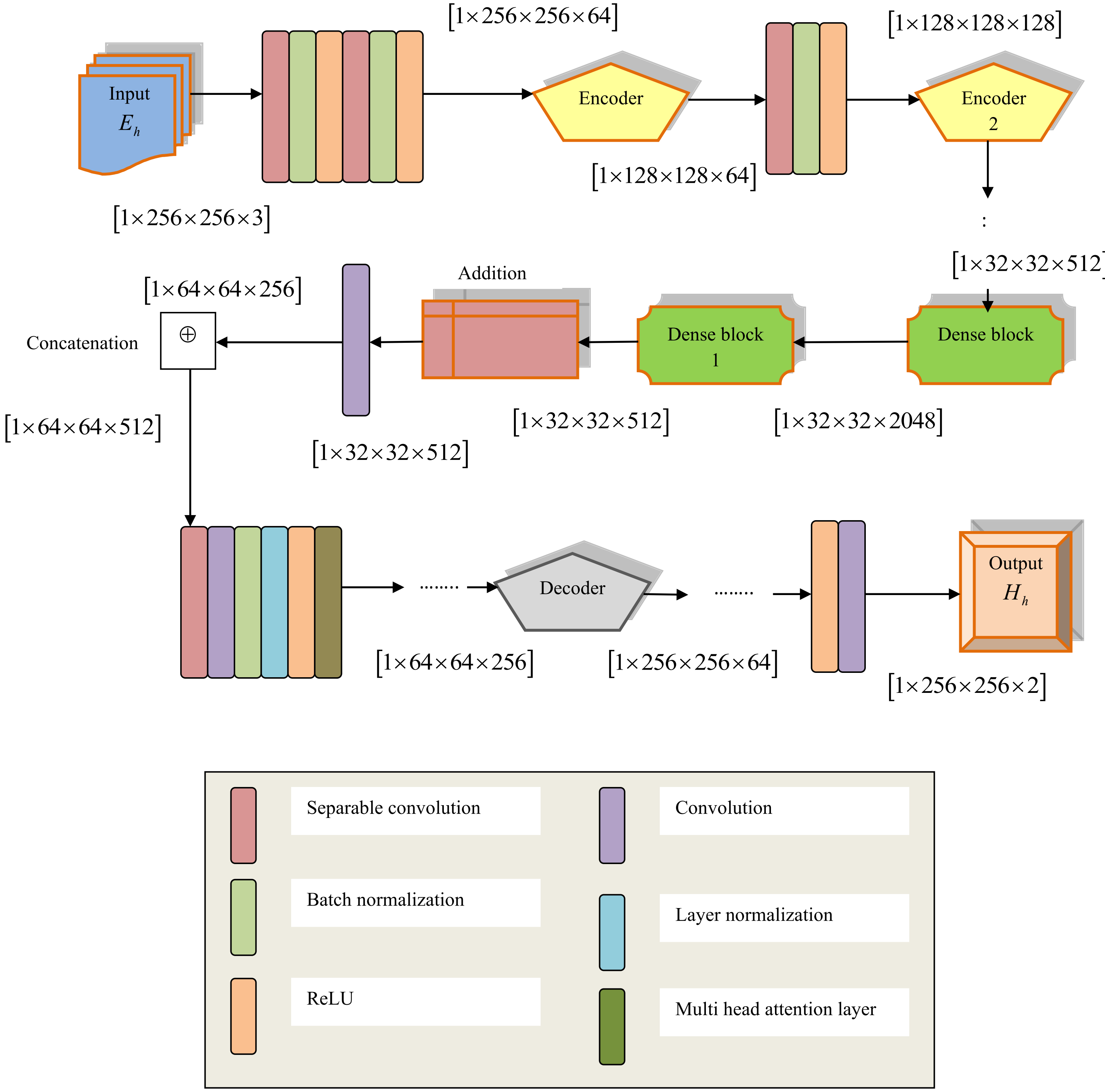

Figure 3. Architecture of TBConvL-Net

d) Feature extraction from lesion segmented output

International Journal of Applied Mathematics
Volume 38 No. 6s, 2025
ISSN: 1311-1728 (printed version); ISSN: 1314-8060 (on-line version)

This scenario involves converting raw image data to meaningful and quantifiable attributes, that is effectively used for tasks, such as classification. Here, segmented output H_h is fed towards extraction of features, where LIFT and statistical features are extracted.

i) LIFT

LIFT [24] comprises three components, such as detector, orientation estimator, and descriptor**.** This process involves learning features from training data, that allows it to extract texturally significant patches that are matched across different images. The descriptor is trained by dropping sum of loss for pairs of corresponding patches $(d_\varepsilon^1, d_\varepsilon^2)$ and loss for pairs of non-corresponding patches $(d_\varepsilon^1, d_\varepsilon^3)$. Loss of pair $(d_\varepsilon^c, d_\varepsilon^e)$ is termed as hinge embedding loss of Euclidean distance among description vectors. This is formulated as below,

$$\mathrm{T}_d(d_\varepsilon^c, d_\varepsilon^e) = \begin{cases} \left\| f_q(d_\varepsilon^c) - f_q(d_\varepsilon^e) \right\|_2 & \textit{for positive pairs} \\ \max\left(0, \mathrm{M} - \left\| f_q(d_\varepsilon^c) - f_q(d_\varepsilon^e) \right\|_2\right) & \textit{for negative pairs} \end{cases} \quad (20)$$

Herein, $\mathrm{M} = 4$ indicates embedding margin, $\|.\|_2$ is Euclidean distance, $f(.)$ indicates descriptor, as well as q is its parameter. The orientation estimator represents the orientation and Structure-from-Motion (SfM) is utilized to find image location. The orientation descriptor loss is thus formulated as,

$$\mathrm{T}_o(B^1, o^1, B^2, o^2) = \left\| f_g(\mathrm{N}(B^1, o^1)) - f_g(\mathrm{N}(B^2, o^2)) \right\|_2 \quad (21)$$

wherein, $\mathrm{N}(B, o)$ is patch centered on o after orientation correction. The minimization of loss by detector is given by,

$$\mathrm{T}_{de}(B^1, B^2, B^3, B^4) = \kappa \mathrm{T}_{cl}(B^1, B^2, B^3, B^4) + \mathrm{T}_{pa}(B^1, B^2) \quad (22)$$

wherein, hyper-parameter balancing dual terms in summation is κ, training quadruplets corresponding same physical point is B^1, B^2, corresponding to varying SfM points is B^1, B^3, and non-feature point location is B^4. Finally, LIFT trains image using multiple patches from different images and brings the similar textures closer in the feature space. Thus, the segmented resultant H_h is applied with LIFT to gain textural image I_h.

ii) Statistical features

Statistical features [25] are numerical measures that capture the distribution, relationships, and variability of data values within an image. Here, extracted statistical features include entropy, mean, and skewness. Textural image I_h is applied with the statistical features to form feature vector J_h.

-Entropy: This measures the segmented image information and amount of disorder in system [25]. This reflects complexity and randomness of pixel intensity values. Increased probability

Received: August 04, 2025

International Journal of Applied Mathematics
Volume 38 No. 6s, 2025
ISSN: 1311-1728 (printed version); ISSN: 1314-8060 (on-line version)

of abnormality prevails in images with larger asymmetry with widely differing entropy. The entropy feature is formulated as below,

$$J_{h1} = \sum_{p=0}^{\mathrm{K}-1} \rho(p) * \log_2 \left[\rho(p)\right] \tag{23}$$

Herein, total grey levels are K, and p is grey level in image.

-Skewness: This represents the degree of symmetry in the distribution of the specified feature relative to the mean [25]. It is calculated using the following equation.

$$J_{h2} = J_{h3}^{-3} \left[\sum_{p=0}^{\mathrm{K}-1} (p-\nu)^3 * \rho(p) \right] \tag{24}$$

where, J_{h3} is mean value.

-Mean: This is the fundamental statistical feature and represents data concentration of distribution [25]. This shows the average intensity value of pixels within image and measures overall gray level of image. The mean term is formulated as below,

$$J_{h3} = \sum_{p=0}^{\mathrm{K}-1} p * \rho(p) \tag{25}$$

Hence, the feature vector is termed as J_h, that is represented as,

$$J_h = \left\{ J_{h1}, J_{h2}, J_{h3} \right\} \tag{26}$$

e) Healthcare classification using DHA-Net

Healthcare classification refers to the use of image processing methods to categorize medical data, such as image into predefined classes, like healthy or diseased. It plays a critical role in assisting clinical decision-making by automatically identifying patterns or abnormalities in medical data, thereby improving the efficiency of diagnosis and treatment planning. In healthcare classification, the feature vector J_h is applied as input to DHA-Net [26] to differentiate between healthy and diseased tissues in medical image. The architecture of DHA-Net is given below,

i) DHA-Net

DHA-Net [26] is a DL model that integrates attention mechanism with higher-order pooling layer. It is built upon ResNet-18 architecture, at which Effective Attention Modules (EAM) are incorporated within residual blocks to enhance feature weights via channel attention learning. High order pooling layers are employed for capturing higher order statistical, complex information from input images.

EAM: These mechanisms are widely used in both vision based and language related applications. Here, the Squeeze-and-Excitation (SENet) module serves as channel attention component, upon which EAM-Net is built. This performs one-dimensional convolution using

International Journal of Applied Mathematics
Volume 38 No. 6s, 2025
ISSN: 1311-1728 (printed version); ISSN: 1314-8060 (on-line version)

conventional kernel size, applied on convolutional feature maps after global average pooling. The sigmoid activation function is then utilized for scaling normalized range values. The procedure involved in using attention module include the following,

- ***No dimension reduction***

As resultant of basic convolutional block is $R \in Y^{r \times s \times t}$, where amount of channels is r, width is s, and height is t. Channel weight is formulated by,

$$\lambda = \omega\left(\vartheta\left\{\varpi_1, \varpi_2\right\}\left(\ell(\theta)\right)\right) \tag{27}$$

wherein, sigmoid function is given as ω, and $\ell(\theta)$ is global average pooling, that is represented as,

$$\ell(\theta) = \frac{1}{st} \sum_{o=1,\xi=1}^{s,t} R_{:,o,\xi} \tag{28}$$

Considering, $\upsilon = \ell(\theta)$, then $\vartheta\left\{\varpi_1, \varpi_2\right\}$ is,

$$\vartheta\left\{\varpi_1, \varpi_2\right\}(\upsilon) = s_2 \operatorname{Re} LU(s_1 \upsilon) \tag{29}$$

where, weights are s_1, s_2. Here, there is no explicit connection among channels and individual weights, instead, channel weights are found solely via fully connected layer. EAM performs single dimensional convolution having Υ feature dimension, wherein Υ is measured from local channel interactions.

- ***Local cross channel interaction***

Local channel interactions are significant, as they contribute to validate the effectiveness of the module. A 1D convolution on feature υ with kernel dimension Υ captures cross channel interactions by,

$$\lambda = \omega\left(\mathrm{H}_{\Upsilon}(\upsilon)\right) \tag{30}$$

Here, one dimensional convolution is H.

Higher order pooling module: This approach is same as first order pooling, as it captures statistical information based on feature sets. High order covariance pooling, derived from first order pooling is proven beneficial in many computer vision tasks.

- ***Higher order normalization***

Considering input features $\mathrm{E} \in Y^{r \times w \times z}$, where w is width as well as z is height of input feature map. Hence, overall feature map is indicated by,

$$\square = \iota(\mathrm{E}; w, r) \tag{31}$$

ISSN: 1311-1728 (printed version); ISSN: 1314-8060 (on-line version)

wherein, ι indicates CNN feature mapping, as well as r is deviation. Herein, feature map $\square \in Y^{r\times w\times z}$ is altered to λ -dimensional feature matrix $\square \in Y^{\lambda\times \mathrm{X}}$, where $\mathrm{X} = z\times w$ features. Next, covariance matrix is formulated as,

$$\mathrm{Z} = \square\,\square\,\square^{T} \tag{32}$$

Here, $\square$ specifies identity matrix, and T is matrix transpose. Hence, covariance matrix after eigen value decomposition application is,

$$\mathrm{Z} \to (C,\Psi), \mathrm{Z} = C\Psi C^{T} \tag{33}$$

wherein, $\Psi = di(s_1....s_\lambda)$ is diagonal matrix, at which $s_b (b = 1....\lambda)$ represents eigen values. Moreover, orthogonal matrix C is $o_1...o_\lambda$. Matrix power operation Z is,

$$(C,\Psi) \to K, K = \mathrm{Z}^{0.5} = Cy(\Psi)C^{T} \tag{34}$$

wherein, $y(\Psi) = \sqrt{di(s_1....s_\lambda)}$. This shows that covariance matrix accomplishes well on value of 0.5.

- ***Covariance normalization***

Decomposition of eigen value is important in high order pooling layer calculations. Here, Newton-Schultz iteration (NSI) is used to find computations, this is given by,

$$L_d = \frac{1}{2} L_{d-1}(3\square - K_{d-1}L_{d-1}) \tag{35}$$

$$K_d = \frac{1}{2} K_{d-1}(3\square - K_{d-1}L_{d-1}) \tag{36}$$

These equations are appropriate for GPU computations, that is found using normal matrix multiplications. Moreover, solution by applying NSI is formed as,

$$\mathrm{Z}' = \frac{1}{t(\mathrm{Z})}\mathrm{Z} \tag{37}$$

Herein, trace of matrix is $t(\mathrm{Z})$, where effect of above equation is balanced by,

$$\mathrm{Z} = \sqrt{t(\mathrm{Z})L_d} \tag{38}$$

Thus, the classified output from DHA-Net is given by X_h. Figure 4 shows architecture of DHA-Net.

Received: August 04, 2025

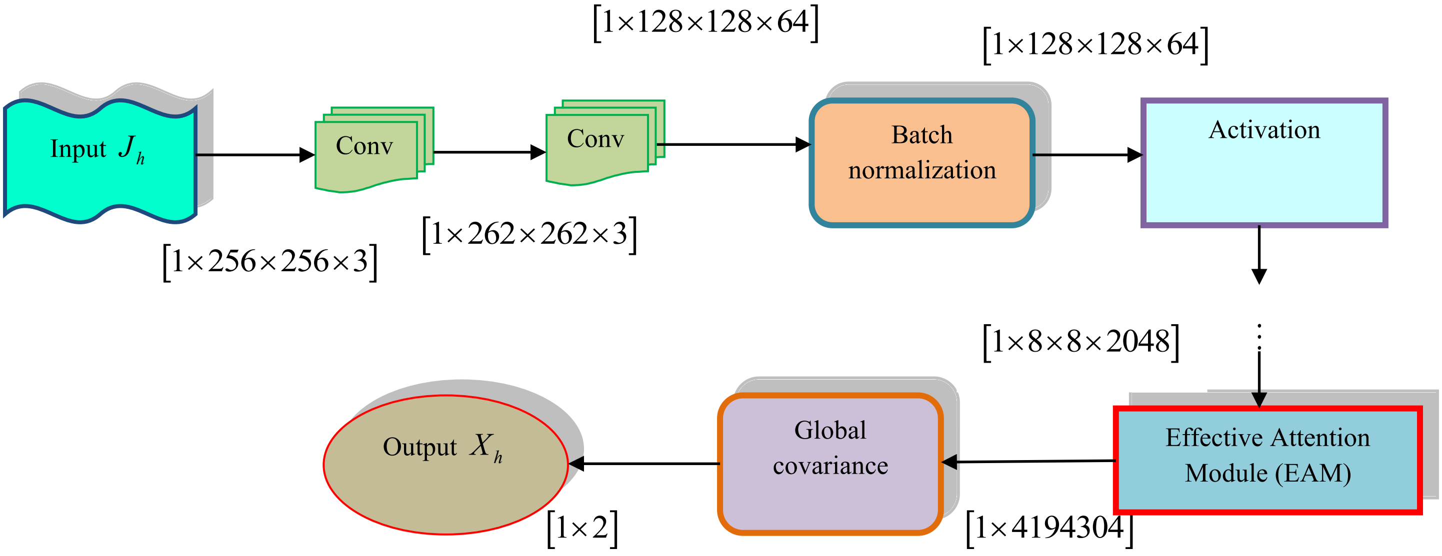

Figure 4. Architecture of DHA-Net

ii) Training of DHA-Net by FFbOA

Training a neural network is crucial for enhancing performance, learning efficiency, and generalization. This process involves adjusting parameters of network for minimizing loss function, which quantifies discrepancy among predicted and actual outputs. Here, DHA-Net is tuned by FFbOA, which is formed by the hybridization of FbOA [27] and FC [28]. FbOA [27] is the population-based metaheuristic optimization algorithm that is inspired by dynamic strategies of football team. This includes flexibility and resilience in football, distribution of ball, completion passes, moves, and frail teamwork. This optimization algorithm thus helps to solve the given problem based on the activities adjusted in football game. Simultaneously, FC [28] is the branch of mathematical analysis generalizing the concept of derivatives and integrals to non-integer or fractional orders. FC is better than classical calculus, as classical calculus deals only with integrals and derivatives of integer orders, wherein FC computes in all derivative orders of function. Thus, the FFbOA balances the problematic strategies and gives a solution for resolving real world scenarios. Algorithmic procedure of FFbOA is as given below,

-Solution encoding: This is applied to identify optimum position within search space S_{pa}, given by,

$$S_{pa} = [1 \times \varsigma_p] \tag{39}$$

where, learning parameter of DHA-Net is ς_p.

Step 1: Initialization

The initialization in FbOA sets up the problem-solving environment, where potential solutions are treated as players on a football field. Here, population size, and maximal number of iterations are initiated along with decision variables. In FbOA, each agent represents a player on football team, and the algorithm simulates the collaborative effort of team working together towards a common objective, identifying the optimal solution.

Step 2: Evaluating fitness

Variation between targeted and DHA-Net resultant is utilized to find fitness solution. The minimum MSE value brings suitable fitness for solving optimization problems, which is formulated by,

$$N_f = \frac{1}{x}\sum_{h=1}^{x}\left[X_{ta} - X_h\right]^2 \tag{40}$$

wherein, fitness is N_f, overall image is x, targeted output is X_{ta}, and DHA-Net resultant is X_h.

Step 3: Exploration phase

In FbOA, one of the players performs his pass with some speed velocity in football game is the assumptions made in exploration phase. This variation in speed is necessary to balance the exploitation and exploration scenario for avoiding the trapping in local optimum. Then, based on this phase, the updated solution at iteration $(u+1)$ is given by,

$$Q(O(u+1)) = v \tag{41}$$

Herein, $Q(O(u+1))$ is updated solution or state at iteration $(u+1)$, and v is player as agent involved in optimization process. Then, the football velocity of each player is represented by,

$$Q_{vu} = A_{f\max}\left(d_{sx}.a_{sx}\left[E_f - A_{f\min}\right] + \psi.d_{sy}.a_{sy}\left[B_f - A_{f\min}\right]\times\cos\left(\frac{\pi}{u}\right)\right) \tag{42}$$

Herein, Q_{vu} is player's velocity at iteration u, $A_{f\max}$ and $A_{f\min}$ are maximal force indicating upper limit of velocity and minimal force indicating lower limit of velocity, a_{sx} and a_{sy} are acceleration factors generating speed variations, d_{sx} and d_{sy} are coefficients indicating influence of various directions in search space, E_f is external force, B_f is best force, ψ is random number, and $\cos\left(\frac{\pi}{u}\right)$ indicates velocity in accordance to number of iterations for balancing exploitation and exploration. Also, the best force is updated by the below formula,

$$B_f = \frac{1}{f_e}\sum_{t=0}^{f_e}\left(\frac{A^{t^2}_{f\max}}{(2t+1)^2}\right) \tag{43}$$

wherein, f_e is exponential factor increasing from 0 to 1, $(2t+1)^2$ is normalization term for controlling update rate, and $A^{t^2}_{f\max}$ specifies search focus on promising regions at iterations proceed.

International Journal of Applied Mathematics
Volume 38 No. 6s, 2025
ISSN: 1311-1728 (printed version); ISSN: 1314-8060 (on-line version)

Step 4: Exploitation phase

In exploitation phase, best or nearly best solution is attained by tuning FbOA in this phase. Here, more rewarding areas are focused in this mechanism and the update rule to adjust the agent position is given as below,

$$Q(O(u+1)) = Q_v + c_p.Q(O(u)) + f_e.\sin\left(\frac{\pi}{u}\right) \tag{44}$$

Substitute $Q(O(u))$ on both sides,

$$Q(O(u+1)) - Q(O(u)) = Q_v + c_p.Q(O(u)) + f_e.\sin\left(\frac{\pi}{u}\right) - Q(O(u)) \tag{45}$$

Herein, $Q(O(u+1))$ is updated position or solution at iteration $(u+1)$, Q_v is current force or position, c_p is control parameter adjusting balance among new and current position, $Q(O(u))$ is current state or position at iteration u, and $\sin\left(\frac{\pi}{u}\right)$ indicates sinusoidal modulation for enhancing convergence speed towards optimum solution.

Then apply FC to Eq. (45),

$$D^m\left[Q(O(u+1))\right] = Q_v + c_p.Q(O(u)) + f_e.\sin\left(\frac{\pi}{u}\right) - Q(O(u)) \tag{46}$$

$$Q(O(u+1)) - m.Q(O(u)) - \frac{1}{2}m.Q(O(u-1)) - \frac{1}{6}(1-m)Q(O(u-2)) - \frac{1}{24}m(1-m)(2-m)Q(O(u-3))$$
$$= Q_v + c_p.Q(O(u)) + f_e.\sin\left(\frac{\pi}{u}\right) - Q(O(u))$$

(47)

$$Q(O(u+1)) = Q(O(u))\left(m + c_p - 1\right) + \frac{1}{2}m.Q(O(u-1)) + \frac{1}{6}(1-m)Q(O(u-2)) + \frac{1}{24}m(1-m)(2-m)Q(O(u-3))$$
$$+ Q_v + f_e.\sin\left(\frac{\pi}{u}\right)$$

(48)

The above solution is updating equation for training DHA-Net.

Step 5: Re-evaluation of fitness

Fitness is reevaluated based on Eq. (40) till attaining best possible solution required for network training.

Step 6: Termination

Algorithmic procedure is terminated after obtaining best solution. Algorithm indicating pseudocode of FFbOA is given below.

International Journal of Applied Mathematics
Volume 38 No. 6s, 2025
ISSN: 1311-1728 (printed version); ISSN: 1314-8060 (on-line version)

Algorithm 1. Pseudocode of FFbOA

	Start FFbOA
	Input: Search space S_{pa}, and population member v.
	Output: Updated solution $Q(O(u+1))$
	Initialize dimension of population and maximal iteration.
	Find fitness by Eq. (40).
	Exploration scenario:
	Position of player is given based on Eq. (41).
	The football velocity is updated based on Eq. (42).
	The best force is updated by Eq. (43).
	Exploitation scenario:
	Position of player is given by Eq. (44)
	Applying FC in FbOA.
	Updating solution by Eq. (48)
	Re-evaluating fitness
	Best solution is obtained
	End

Thus, attained update solution trains the network for privacy preserved healthcare classification, ensuring better efficiency of the model in lesser training time.

3.2 Aggregation at global Blockchain enabled cloud server

The aggregation of data is performed at a global cloud server integrated with blockchain technology, ensuring secure, decentralized, and transparent processing. After the appropriate healthcare classification, the classified outputs are assigned as weights and updated in the global system with blockchain enabled cloud server. Here, the medical images are appropriately classified and the assigned weights are indicated as D_1, D_2, D_3. These weights from different local training data or image are aggregated and the weights are averaged as D. Also, assigning weights during data aggregation at a global blockchain-enabled cloud server is essential to ensure that the aggregation reflects the data quality, importance, or trustworthiness across diverse sources. Figure 5 shows the representation of aggregation.

International Journal of Applied Mathematics
Volume 38 No. 6s, 2025
ISSN: 1311-1728 (printed version); ISSN: 1314-8060 (on-line version)

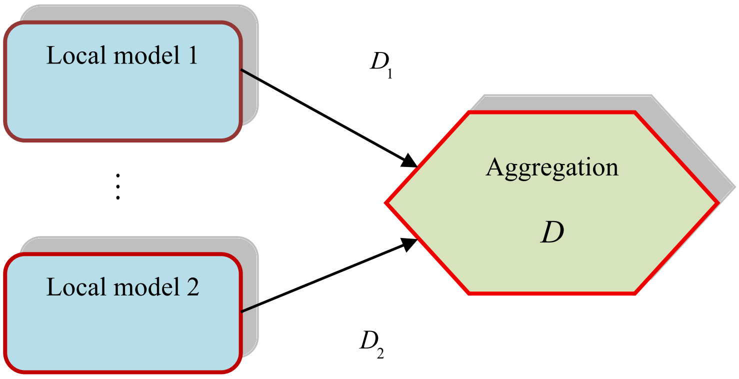

Figure 5. Pictorial representation of aggregation

3.3 Applying global model on every local node

In FC, many local devices or nodes train the model without sharing of raw data. Each local node trains the model on its own data and sends learned parameters to central server. Server aggregates these parameters by averaging them to form global model. This is then distributed back to each local node, where it is either directly applied for inference or used as starting point for further local training. This process continues iteratively, allowing all nodes to benefit from collective intelligence of network while preservation of data privacy and minimizing communication overhead. Thus, finally averaged weights are updated to every local model for better privacy enhancement.

4. Results and Discussions

Performance of FFbOA_DHA-Net for blockchain enabled FL based privacy preserved healthcare classification is assessed in this section.

4.1 Experimental setup

The FFbOA_DHA-Net is implemented in the Python tool with IDRiD [21].

4.2 Dataset description

The dataset utilized in this work is IDRiD [21] with images showing the detailed information on the severity of diabetic retinopathy and diabetic macular edema, making the dataset highly valuable for evaluating and developing image analysis algorithms aimed at early detection of diabetic retinopathy. The disease grading, optic disc and fovea detection, as well as lesion segmentation, are tasks performed in this dataset. The images available in this dataset is in the format of JPG and TIF files. There are 81 images in segmentation phase, 516 images in disease grading, and 516 images in the localization phase.

4.3 Evaluation measures

Evaluation metrics used are loss, MSE, F1-measure, RMSE, and MAP.

4.3.1 Loss

Received: August 04, 2025

International Journal of Applied Mathematics
Volume 38 No. 6s, 2025
ISSN: 1311-1728 (printed version); ISSN: 1314-8060 (on-line version)

The variation among actual values and predicted values generated by model is referred as loss, which quantifies prediction error of model. A lower loss value indicates that predictions of model nearer to actual values represent better performance. Minimizing this loss at training is essential, as it guides the optimization to adjust model parameters, like weights and biases towards achieving higher accuracy and generalization.

4.3.2 MSE

MSE [29] is used to calculate the average of the squared differences between the actual and predicted values. The MSE value is the fitness value and this is shown in Eq. (40).

4.3.3 RMSE

RMSE [29] is defined as the square root of the mean of the squared differences between the expected and predicted outcomes. It is formed by square root of MSE term, which is expressed as below,

$$N_{rm} = \sqrt{N_f} = \sqrt{\frac{1}{x}\sum_{h=1}^{x}\left[X_{ta} - X_h\right]^2} \tag{49}$$

Here, N_{rm} indicates RMSE.

4.3.4 MAP

MAP [30] evaluates the precision of predictions at various points in ranked output, focusing on both the order and correctness of the results. It specifies the models that assign higher ranks to correct predictions within the output list, and is formulated by,

$$N_{map} = \frac{1}{x}\sum_{h=1}^{x} A_{pavg} \tag{50}$$

Herein, N_{map} indicates MAP, x is total count of samples, and A_{pavg} is average precision.

4.3.5 F1-score

F1-score [31] represents a balanced measure that combines both precision and recall, making it particularly suitable for imbalanced datasets by accounting for both normal and abnormal instances. It is calculated using following formula,

$$N_{fs} = \frac{2 \times A_p \times A_r}{A_p + A_r} \tag{51}$$

Herein, F1-score is N_{fs}, precision is A_p, as well as recall is A_r.

4.4 Experimental resultant

Experimental outcomes of classified images are given in figure 6. Figure 6 a), b), c), and d) indicates input image-1, 2, 3, and 4. Figure 6 e), f), g), and h) shows filtered or pre-processed image-1, 2, 3, and 4. Figure 6 i), j), k), and l) indicates segmented image-1, 2, 3, and 4. Figure

International Journal of Applied Mathematics
Volume 38 No. 6s, 2025
ISSN: 1311-1728 (printed version); ISSN: 1314-8060 (on-line version)

6 m), n), o), and p) shows LIFT featured image-1, 2, 3, and 4. Figure 6 q), r), s), and t) specifies output image-1, 2, 3, and 4.

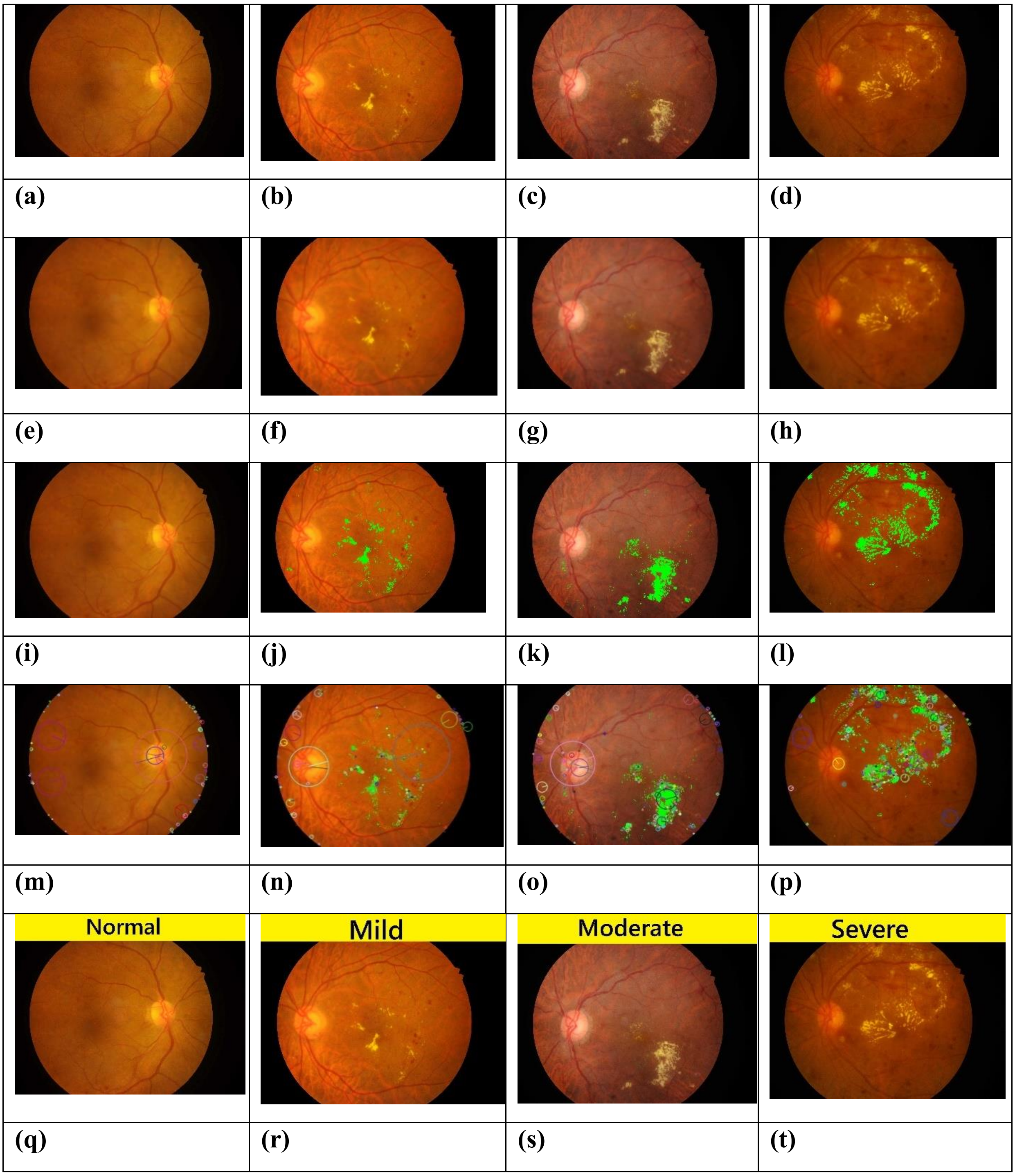

Figure 6. Experimental image outputs, a) input image-1, b) input image-2, c) input image-3, d) input image-4, e) pre-processed image-1, f) pre-processed image-2, g) pre-processed image-3, h) pre-processed image-4, i) segmented image-1, j) segmented image-2, k) segmented image-3, l) segmented image-4, m) LIFT featured image-1, n) LIFT featured

ISSN: 1311-1728 (printed version); ISSN: 1314-8060 (on-line version)

image-2, o) LIFT featured image-3, p) LIFT featured image-4, q) output image-1, r) output image-2, s) output image-3, t) output image-4

4.5 Training loss

Training loss is the key concept measuring the assessment of model in performing during training scenario by quantifying the difference among predictions of model and actual target values. The goal of this graph is to ensure the minimization of loss at training time to make accurate predictions. Figure 7 shows the training loss graph in terms of epoch. Here, training loss is 0.288 for epoch of 0, 0.130 for epoch of 20, 0.058 for epoch of 40, 0.026 for epoch of 60, 0.012 for epoch of 80, and 0.005 for epoch of 100.

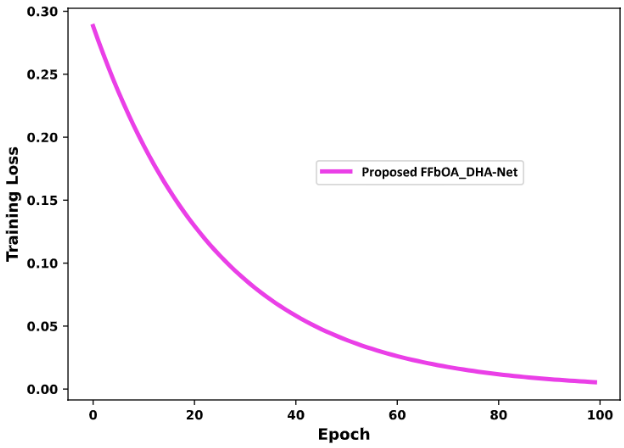

Figure 7. Training loss

4.6 Comparative assessment

Comparative assessment for FFbOA_DHA-Net is carried out with respect to time stamp and training percentage.

4.7 Comparative methods

The comparative methods used for assessment are FL-BETS [8], FedViTBloc [15], CapsNet with IELMs [4], DMFL_Net+DenseNet-169 [18], and proposed FFbOA_DHA-Net.

4.7.1 Based on time stamp

Figure 8 shows comparative assessment in terms of altering time stamp. Figure 8 a) is comparative analysis in terms of RMSE. For time stamp of 20sec, RMSE for FFbOA_DHA-Net is 0.589, wherein other techniques attained RMSE of 0.689, 0.658, 0.640, and 0.617. Figure 8 b) indicates the loss enabled comparative assessment. When time stamp is considered as 20sec, then loss for FFbOA_DHA-Net is 0.096, wherein other techniques gained loss of 0.152, 0.138, 0.128, and 0.112. Figure 8 c) shows comparative assessment with respect to F1-score. The F1-score is 89.99% for FFbOA_DHA-Net, wherein it is 82.24%, 84.04%, 85.34%, and 87.72% for other models while time stamp is 20sec. Figure 8 d) shows comparative assessment in terms of MAP. While time stamp is taken as 20sec, the MAP is 90.67% for FFbOA_DHA-Net, where other models attained MAP of 82.26%, 84.11%,

International Journal of Applied Mathematics
Volume 38 No. 6s, 2025
ISSN: 1311-1728 (printed version); ISSN: 1314-8060 (on-line version)

86.90%, and 88.75%. Figure 8 e) shows the comparison graph in accordance to MSE. The MSE for FFbOA_DHA-Net is 0.347, wherein other methods attained MSE of 0.474, 0.433, 0.410, and 0.381, while time stamp is taken as 20sec.

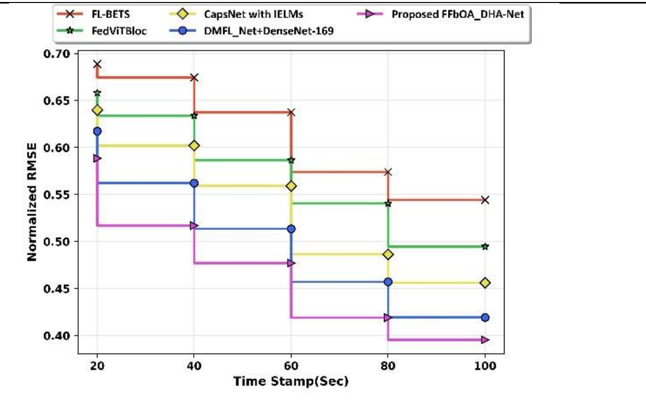

(a)

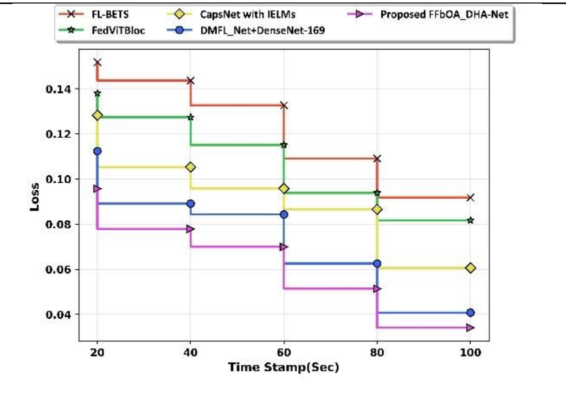

(b)

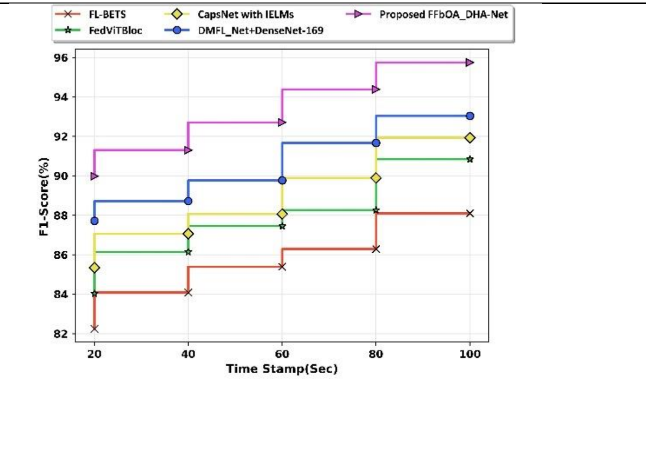

(c)

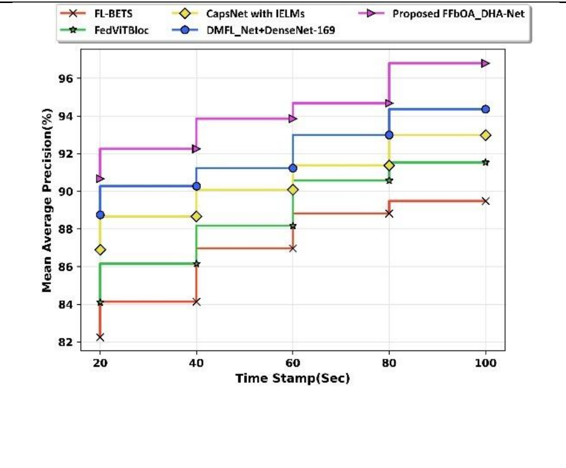

(d)

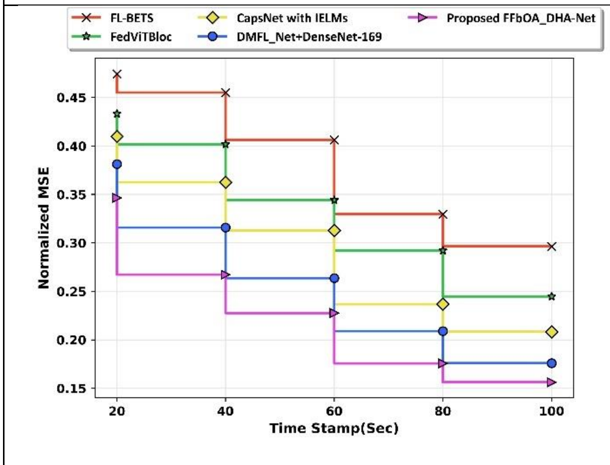

(e)

Figure 8. Comparative assessment with respect to time stamp, a) RMSE, b) loss, c) F1-score, d) MAP, e) MSE

International Journal of Applied Mathematics
Volume 38 No. 6s, 2025
ISSN: 1311-1728 (printed version); ISSN: 1314-8060 (on-line version)

4.7.2 Based on training data

Figure 9 indicates comparative assessment with training data. Figure 9 a) shows comparative analysis on RMSE. For training data of 50%, RMSE for FFbOA_DHA-Net is 0.596, wherein other methods gained RMSE of 0.713, 0.682, 0.647, and 0.614. Figure 9 b) indicates comparative assessment for loss function. For training data of 50%, loss for FFbOA_DHA-Net is 0.085, wherein other models gained loss of 0.168, 0.153, 0.124, and 0.104. Figure 9 c) shows the comparative assessment with respect to F1-score. The F1-score is 89.17% for FFbOA_DHA-Net, wherein it is 81.94%, 83.97%, 84.36%, and 86.01% for other models while training data is 50%. Figure 9 d) shows comparative analysis for MAP. While training data is considered as 50%, the MAP is 90.80% for FFbOA_DHA-Net, where other models attained MAP of 82.47%, 85.07%, 87.89%, and 88.27%. Figure 9 e) shows the comparison graph in accordance to MSE. The MSE for FFbOA_DHA-Net is 0.355, whereas other techniques gained MSE of 0.508, 0.465, 0.418, and 0.377, while training data is considered as 50%.

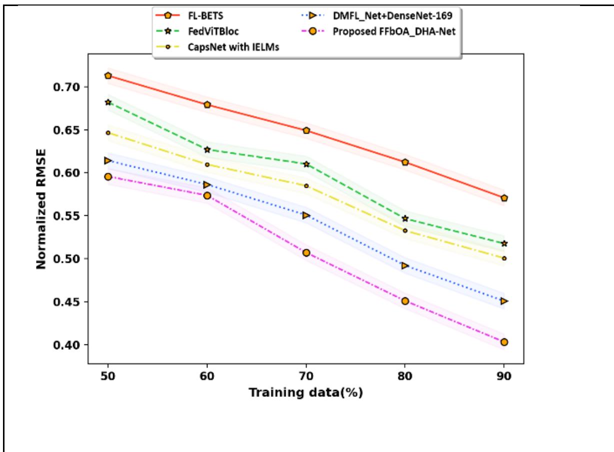

(a)

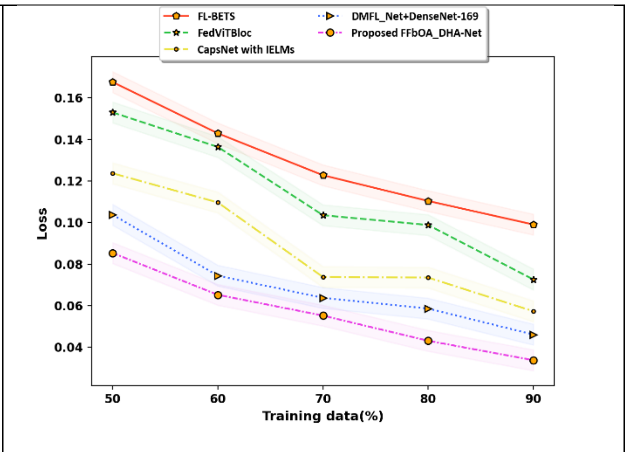

(b)

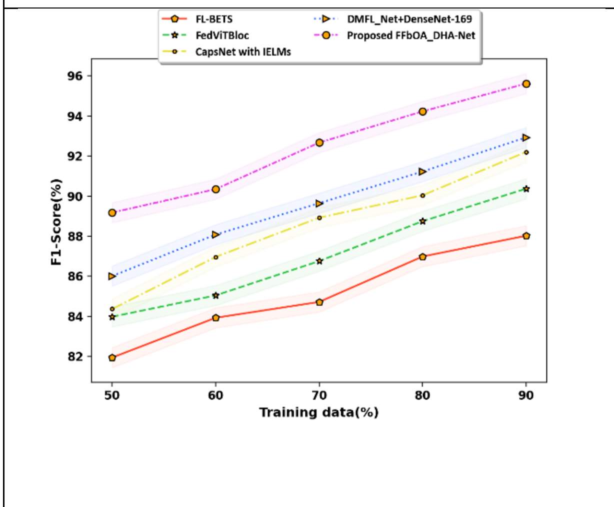

(c)

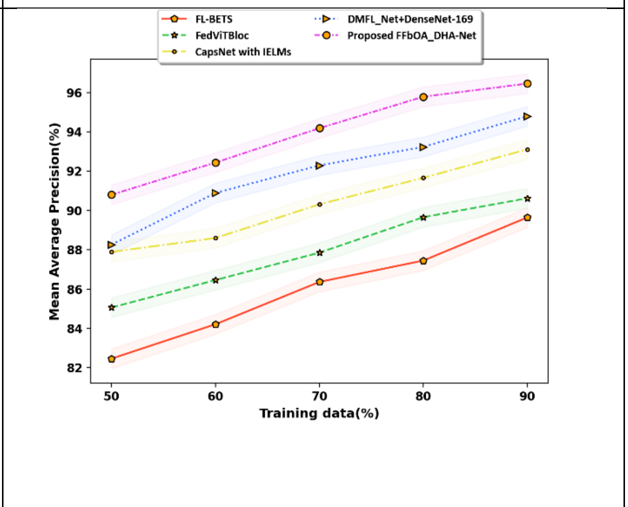

(d)

ISSN: 1311-1728 (printed version); ISSN: 1314-8060 (on-line version)

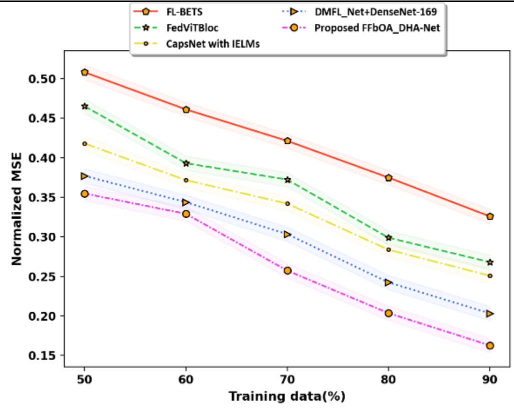

(e)

Figure 9. Comparative assessment by varying training data, a) RMSE, b) loss, c) F1-score, d) MAP, e) MSE

4.8 Comparative Discussion

Table 1 shows comparative discussion of FFbOA_DHA-Net with respect to other techniques, like FL-BETS, CapsNet with IELMs, FedViTBloc, and DMFL_Net+DenseNet-169. Here, the proposed FFbOA_DHA-Net attained RMSE of 0.395, where other models gained RMSE of 0.544, 0.495, 0.456, and 0.419 when time stamp is 100sec. Also, F1-score is 95.75% for FFbOA_DHA-Net, where other techniques attained F1-score of 88.10%, 90.84%, 91.93%, and 93.04% when time stamp is 100sec. Similarly, loss value is 0.034 for FFbOA_DHA-Net when time stamp is 100sec, wherein other models attained loss of 0.092, 0.082, 0.061, and 0.041. Further, when time stamp is 100sec, the FFbOA_DHA-Net gained MAP of 96.81%, where other models attained MAP of 89.49%, 91.54%, 92.98%, and 94.36%. Then, when time stamp is 100sec, the MSE value for other models is 0.296, 0.245, 0.208, and 0.176, wherein FFbOA_DHA-Net gained MSE of 0.156. Moreover, when training percentage is 90%, the RMSE, loss, F1-score, MAP, and MSE is 0.403, 0.034, 95.61%, 96.45%, and 0.163 for proposed FFbOA_DHA-Net. Thus, the superior values of metrics are attained by FFbOA_DHA-Net when time stamp is 100sec. Thus, this model facilitated secure and decentralized model training across multiple healthcare institutions by keeping sensitive patient data confidential, thus ensuring data regulatory compliance.

Table 1. Comparative Discussion

Setups	**Methods /Metrics**	**FL-BETS**	**FedViTBloc**	**CapsNet with IELMs**	**DMFL_Net+DenseNet-169**	**Proposed FFbOA_DHA-Net**
Time stamp=	*RMSE*	0.544	0.495	0.456	0.419	**0.395**
	Loss	0.092	0.082	0.061	0.041	**0.034**

International Journal of Applied Mathematics
Volume 38 No. 6s, 2025
ISSN: 1311-1728 (printed version); ISSN: 1314-8060 (on-line version)

100sec	*F1-score (%)*	88.10	90.84	91.93	93.04	**95.75**
	MAP (%)	89.49	91.54	92.98	94.36	**96.81**
	MSE	0.296	0.245	0.208	0.176	**0.156**
Training data= 90%	*RMSE*	0.571	0.518	0.501	0.451	0.403
	Loss	0.099	0.073	0.057	0.046	0.034
	F1-score (%)	88.02	90.37	92.20	92.93	95.61
	MAP (%)	89.64	90.62	93.11	94.79	96.45
	MSE	0.326	0.268	0.251	0.203	0.163

5. Conclusion

Privacy preservation is crucial in healthcare due to strict regulations and ethical need to safeguard personal health information. A promising approach to achieve this is Blockchain-enabled FL, which ensures data privacy, and security across decentralized healthcare systems. However, ensuring data heterogeneity across different healthcare nodes complicates global model convergence. To address these limitations, FFbOA_DHA-Net is proposed for privacy preserved healthcare classification. Initially, each local node performs local training, wherein training process involves acquisition of image, and then pre-processing is done using midpoint filter. Further, lesion segmentation is performed using TBConvL-Net and then feature extraction is conducted. Finally, healthcare classification is done using DHA-Net, that is optimized using FFbOA, formed by merging FbOA with FC. After local training, the learned weights from various nodes are aggregated and averaged on global server. Then, resulting global model is deployed to each local node to update models using averaged weights. Moreover, the performance of FFbOA_DHA-Net is evaluated using loss, MSE, RMSE, MAP, and F1-score, that obtained superior values of 0.034, 0.156, 0.395, 96.81%, and 95.75%. In future, this model will be further updated with trust and heterogeneity aware decentralized FL framework for privacy preserved healthcare classification.

International Journal of Applied Mathematics
Volume 38 No. 6s, 2025
ISSN: 1311-1728 (printed version); ISSN: 1314-8060 (on-line version)

References

[1] N. Dilawar, M. Rizwan, F. Ahmad and S. Akram, "Blockchain: securing internet of medical things (IoMT)," *International Journal of Advanced Computer Science and Applications,* vol. 10, no. 1, pp. 82-89, 2019.

[2] D. E. Majdoubi, H. E. Bakkali, S. Sadki, Z. Maqour and A. Leghmid, "The systematic literature review of privacy-preserving solutions in smart healthcare environment," *Security and Communication Networks,* vol. 2022, no. 1, p. 5642026, 2022.

[3] M. A. Sahi, H. Abbas, K. Saleem, X. Yang, A. Derhab, M. Orgun, W. Iqbal, I. Rashid and A. Yaseen, "Privacy Preservation in e-Healthcare Environments: A Review," *IEEE Access,* vol. 6, pp. 464-478, 2017.

[4] H. Malik, T. Anees, A. Naeem, R. A. Naqvi and W.-K. Loh, "Blockchain-federated and deep-learning-based ensembling of capsule network with incremental extreme learning machines for classification of COVID-19 using CT scans," *Bioengineering,* vol. 10, no. 2, p. 203, 2023.

[5] V. Stephanie, I. Khalil, M. Atiquzzaman and X. Yi, "Trustworthy privacy-preserving hierarchical ensemble and federated learning in healthcare 4.0 with blockchain," *IEEE Transactions on Industrial Informatics,* vol. 19, no. 7, pp. 7936-7945, 2022.

[6] G. Bian, W. Qu and B. Shao, "Blockchain-based trusted federated learning with pre-trained models for COVID-19 detection," *Electronics,* vol. 12, no. 9, p. 2068, 2023.

[7] Y. Qu, L. Gao, T. H. Luan, Y. Xiang, S. Yu, B. Li and G. Zheng, "Decentralized privacy using blockchain-enabled federated learning in fog computing," *IEEE Internet of Things Journal,* vol. 7, no. 6, pp. 5171-5183, 2020.

[8] A. lakhan, M. A. Mohammed, J. Nedoma, R. Martinek, P. Tiwar, A. Vidyarth, A. Alkhayyat and W. Wang, "Federated-learning based privacy preservation and fraud-enabled blockchain IoMT system for healthcare," *IEEE journal of biomedical and health informatics,* vol. 27, no. 2, pp. 664-672, 2022.

[9] H. Kassem, D. Alapatt, P. Mascagni, C. AI4SafeChole, A. Karargyris and N. Padoy, "Federated cycling (fedcy): Semi-supervised federated learning of surgical phases," *IEEE transactions on medical imaging,* vol. 42, no. 7, pp. 1920-1931, 2022.

[10] S. Nazir and M. Kaleem, "Federated learning for medical image analysis with deep neural networks," *Diagnostics,* vol. 13, no. 9, p. 1532, 2023.

[11] M. U. Alam and R. Rahmani, "Federated semi-supervised multi-task learning to detect covid-19 and lungs segmentation marking using chest radiography images and raspberry pi devices: An internet of medical things application," *Sensors,* vol. 21, no. 15, p. 5025,

ISSN: 1311-1728 (printed version); ISSN: 1314-8060 (on-line version)

2021.

[12] Y. Chen, J. Wang, C. Yu, W. Gao and X. Qin, "Fedhealth: A federated transfer learning framework for wearable healthcare," *IEEE Intelligent Systems,* vol. 35, no. 4, pp. 83-93, 2020.

[13] P. C.-R. Shyu, K. T. Putra, H.-C. Chen, Y.-Y. Tsai, K. S. M. T. H. W. Jiang and Z.-Y. Shae, "A systematic review of federated learning in the healthcare area: From the perspective of data properties and applications," *Applied Sciences,* vol. 11, no. 23, p. 11191, 2021.

[14] B. Ristevski and M. Chen, "Big data analytics in medicine and healthcare," *Journal of integrative bioinformatics,* vol. 15, no. 3, p. 20170030, 2018.

[15] G. C. Amaizua, A. M. V. V. Saia, S. Bwardwaj, D.-S. Kim, M. Siddula and Y. Li, "FedViTBloc: Secure and privacy-enhanced medical image analysis with federated vision transformer and blockchain," *High-Confidence Computing,* p. 100302, 2025.

[16] A. AV. Voulodimos, E. EP. Protopapadakis, I. IK. Katsamenis, A. AD.Doulamis and N. ND.Doulamis, "Deep learning models for COVID-19 infected area segmentation in CT images," in *Proceedings of the 14th PErvasive Technologies Related to Assistive Environments Conference*, 2021.

[17] M. A. Rahman, M. S. Hossain, M. S. Islam, N. A. Alrajeh and G. Muhammad, "Secure and provenance enhanced internet of health things framework: A blockchain managed federated learning approach," *ccess,* vol. 8, pp. 205071-205087, 2020.

[18] H. Malik, A. Naeem, R. A. Naqvi and W.-K. Loh, "DMFL_Net: A federated learning-based framework for the classification of COVID-19 from multiple chest diseases using X-rays," vol. 23, no. 2, p. 743, 2023.

[19] R. Saidi, I. Rahmany, S. Dhahri and T. Moulahi, "A Privacy-Enhanced Framework for Chest Disease Classification using Federated Learning and Blockchain," *IEEE Access,* 2024.

[20] R. Durga and E. Poovammal., "Fled-block: Federated learning ensembled deep learning blockchain model for covid-19 prediction," *Frontiers in Public Health,* vol. 10, p. 892499, 2022.

[21] "Indian Diabetic Retinopathy Image Dataset (IDRiD)," [Online]. Available: https://ieee-dataport.org/open-access/indian-diabetic-retinopathy-image-dataset-idrid. [Accessed June 2025].

[22] E. S. and D. E. , "New nonlinear filtering strategies for eliminating short and long tailed noise in images with edge preservation properties," *International Journal of Information and Communication Engineering,* vol. 4, no. 3, pp. 175-181, 2008.

[23] S. Iqbal, T. M. Khan, S. S. Naqvi, A. Naveed and E. Meijering, "TBConvL-Net: A hybrid deep learning architecture for robust medical image segmentation," *Pattern Recognition,* vol. 158, p. 111028, 2025.

[24] K. M. Yi, E. Trulls, V. Lepetit and P. Fua, "Lift: Learned invariant feature transform," 2016.

[25] V. Lessa and M. Marengoni, "Applying artificial neural network for the classification of breast cancer using infrared thermographic images," in *Proceedings of International conference on computer vision and graphics, Cham: Springer International Publishing*, 2016.

[26] M. Waqas, A. Ahmed, T. Maul and I. Y. Liao, "Enhancing breast cancer histopathological image classification using attention-based high order covariance pooling," *Neural Computing and Applications,* vol. 36, no. 36, pp. 23275-23293, 2024.

[27] E.-S. M. El-Kenawy, F. H. Rizk, A. M. Zaki, M. E. Mohamed, A. Ibrahim, A. A. Abdelhamid, N. Khodadadi, E. M Almetwally and M. M. Eid, "Football optimization algorithm (fboa): A novel metaheuristic inspired by team strategy dynamics," *Journal of Artificial Intelligence and Metaheuristics (JAIM),* vol. 8, no. 1, pp. 21-38, 2024.

[28] P. R. Bhaladhare and D. C. Jinwala, "A clustering approach for the l-diversity model in privacy preserving data mining using fractional calculus-bacterial foraging optimization algorithm," *Advances in Computer Engineering,* vol. 2014, no. 1, p. 396529, 2014.

[29] O. E. Obisesan, "Machine Learning Models for Prediction of Meteorological Variables for Weather Forecasting," *Int. J. Environ. Clim. Change,* vol. 14, no. 1, pp. 234-252, 2024.

[30] K. Li, Z. Huang, Y.-C. Cheng and C.-H. Lee, "A maximal figure-of-merit learning approach to maximizing mean average precision with deep neural network based classifiers," in *2014 IEEE International Conference on Acoustics, Speech and Signal Processing (ICASSP)* , 2014.

[31] R. Devi D and S. S. , "Ensemble incremental deep multiple layer perceptron model– sentiment analysis application," *International Journal of Web Information Systems,* vol. 17, no. 6, pp. 714-727, 2021.